

Programma
SHORT TERM MOBILITY 2016

Relazione scientifica
sulle attività svolte nell'ambito del progetto

**CARATTERIZZAZIONE DELLA SEVERITÀ DEGLI INCENDI TRAMITE FUSIONE DI DATI
SATELLITARI OTTICI E RADAR**

Svolte presso:
CNR – IREA, sede di Milano
21st November to 2nd December 2016

Luigi BOSCHETTI
(Department of Natural Resources and Society, University of Idaho, USA)

&

Pietro Alessandro Brivio, Daniela Stroppiana, Ramin Saidiazar (CNR-IREA, Milano)
Antonio Pepe, Fabiana Calo', Pasquale Imperatore (CNR-IREA, Napoli)



University of Idaho
College of Natural Resources
Department of Natural Resources and Society

Proposed activity

Obiettivi: Analisi di dati Sentinel-1A (C band) Synthetic Aperture Radar (SAR), in combinazione con dati ottici Landsat 7-8 e Sentinel-2, per la caratterizzazione dello stato della vegetazione post-incendio, e per il monitoraggio della riforestazione successiva all'incendio. Confronto con dati a terra raccolti dall'US Forest Service (USFS) a distanza di 1, 5 e 10 anni da incendi in foresta temperata. Pubblicazione dei risultati.

Attività da svolgere: 1) Identificazione ed acquisizione delle immagini satellitari coincidenti con i siti di misure a terra condotti dall'USFS, e che verranno messi a disposizione del Dr. Boschetti dalla Rocky Mountain Research Station (referente: Dr. Andrew Hudak). I siti includono aree bruciate negli anni 2014-2015, e negli anni 2002-2004, con successive rivisite per monitorare lo stato della vegetazione. 2) Perimetrazione delle aree bruciate verrà condotta su dati Landsat e Sentinel-2. 3) Analisi dei dati SAR all'interno dei perimetri bruciati, sia su aree recenti, che su aree bruciate da circa 10 anni. Verranno analizzati sia l'intensità del ritorno del segnale (backscatter intensity) che le componenti della polarizzazione del segnale (polarimetric decomposition). La letteratura preesistente indica che, nella banda C usata da Sentinel-1, l'intensità del segnale satura in corrispondenza di valori di biomassa relativamente bassi, ma che è possibile correlare la polarizzazione del segnale ai cambiamenti strutturali indotti dal fuoco in foresta 4) confronto con i dati a terra e documentazione dei risultati.

Descrizione del progetto: Il progetto si inquadra negli studi dedicati agli effetti degli incendi sugli ecosistemi forestali, e sullo sviluppo di sistemi per il monitoraggio in remoto di tali effetti. Il lancio dei satelliti della serie Sentinel-1 dell'Agenzia Spaziale Europea (Sentinel 1A, lanciato Aprile 2014 e Sentinel 1B, lanciato Aprile 2016), e la politica di accesso libero ai dati Sentinel deciso dalla Comunità Europea, offre nuove opportunità per l'integrazione di dati SAR nei sistemi di monitoraggio degli incendi, tradizionalmente limitati a dati ottici. Studi precedenti hanno evidenziato il potenziale utilizzo dei dati SAR nella caratterizzazione della severità degli incendi; l'obiettivo del presente progetto è la verifica della potenzialità di combinare dati ottici e radar, conducendo la perimetrazione delle aree con dati ottici, e la caratterizzazione della perdita di biomassa e del cambiamento della struttura della foresta da dati SAR.

Activities performed during the program

1. Theoretical Background

Optical satellite remote sensing has been very successful in the identification of actively burning fires (Giglio et al., 2003; Shroeder et al., 2014; Shroeder et al., 2016) and in mapping burned areas (Tansey et al., 2004; Roy et al., 2008; Stroppiana et al., 2012; Boschetti et al., 2015) at a variety of spatial resolutions and using a variety of sensors. However, research is still ongoing on how to assess fire's effects within burned areas. Information on within-burn variability is not only needed for planning post-fire rehabilitation and remediation, but also to understand the long term effects of fire on ecosystem processes, such as, for example, vegetation recovery and succession.

Fire severity is term used to indicate the magnitude of the effects of fire on the ecosystem; parameters used to estimate fire severity on the field include tree mortality, amount of fuel consumed, loss of organic soil (Key and Benson, 1999). While optical data can be used to provide an indication of severity, by detecting the loss of photosynthetic activity and the presence of char on the ground (Kasischke et al., 2008; De Santis et al., 2009), it remains insensitive to the loss of wooden biomass, and to the structural changes induced by fire on vegetation, especially in forest environments (Roy et al., 2006; Smith et al, 2016).

Radar backscatter, instead, is sensitive both to the presence of wooden biomass, and to its spatial distribution, and there is a long heritage in using radar data for forest mapping, forest degradation monitoring, and biomass estimation (Dobson et al, 1992; LeToan, 1992; Imhoff, 1995; Saatchi et al., 2001). For this reason, radar data have been recently used to estimate post-fire effects (Tanase et al, 2014; Tanase et al., 2015a; Stroppiana et al., 2015; Tanase et al. 2015b; Martins et al., 2016).

The successful launch of the Sentinel 1-A satellite in 2014, followed by Sentinel 1-B in 2016, combined with a global acquisition strategy and a free and open access data policy, provides an unprecedented opportunity to use radar data for systematic forest monitoring, including forest degradation due to fires (Malenovsky et al., 2012; Verhegghen et al., 2016).

The Sentinel-1 satellites are on a near-polar Sun-Synchronous orbit, with a revisit time of 12 days; the main payload is a C-band interferometric radar instrument (Torres et al., 2012). In Wide-Swath mode the instrument operates in dual polarization (HH+HV or VV+VH), with a ground swath of 250km and a ground range resolution of 5m.

As exemplified in figure 1, C-band radar pulses are mostly reflected by the smaller elements of a forest, such as twigs and small branches, thus making Sentinel-1 data unsuitable for direct forest biomass estimation, due to saturation at relatively low level of biomass.

Forest fires, however, rather than the complete loss of above ground biomass, cause (Dickinson and Johnson, 2001):

- loss of leaves and canopy
- loss of smaller branches (stems of dead tree can stand up to 10/15 after a fire)
- loss of understory.

Recent works have therefore presented successful application of polarimetric C-band radar data for the characterization of fire severity (Tanase et al., 2014; Kurum, 2015).

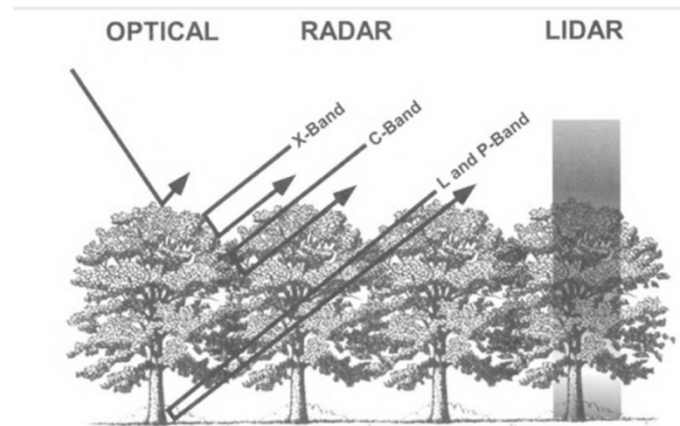


Figure 1: Conceptual scheme of the interaction between electromagnetic radiation and forest canopy as a function of the wavelength. Optical data is mostly sensitive to the spectral properties of leaves, short wave radar data (X, C band, see Table 1) is sensitive to small diameter elements (i.e. twigs and small branches), while longer wavelength radar data (P, L band) penetrates through the canopy and is reflected by larger structures. LiDAR is an active optical instrument, with the ability of tracking the depth of penetration through the open spaces in the canopy, providing information on sub-canopy features.

Table 1: Frequency and wavelength of the portions of the electromagnetic spectrum used for satellite radar Earth observation.

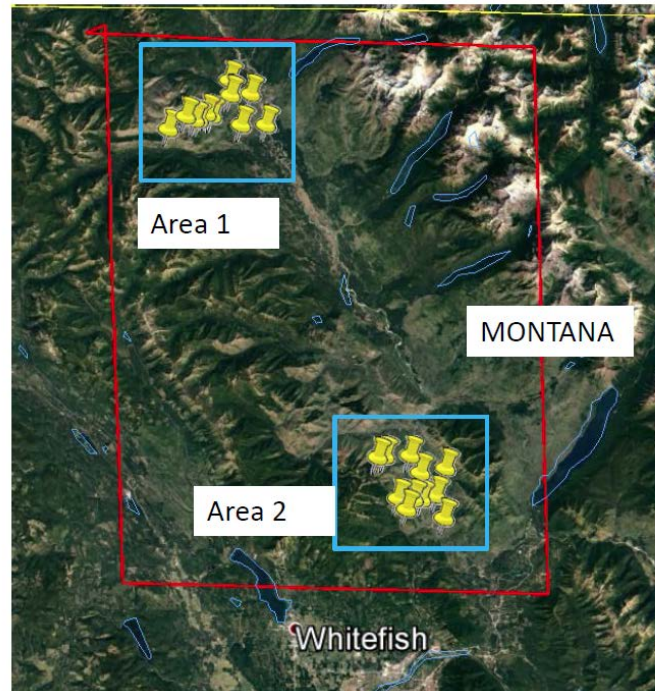
X Band	2.5 to 3.75 cm	12,000 - 8,000 MHz
C Band	3.75 to 7.5 cm	8,000 - 4,000 MHz
L Band	20 to 60 cm	1,500 - 500 MHz
P Band	60 to 120 cm	500 - 250 MHz

2. Preliminary analysis and redefinition of the objectives

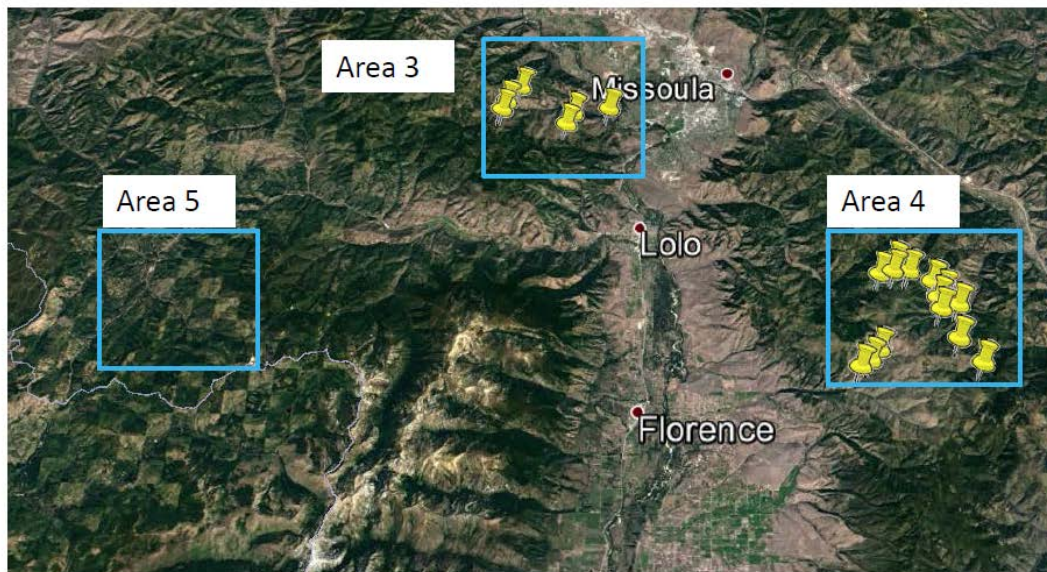
The study was initially designed to make use of the ground data collected by the US Forest Service (A.Hudak P.I.) at repeated intervals on fires occurred in 2004-2005, to assess post-fire vegetation regrowth. Among the available sites in the Pacific Northwest of the United States, 5 burned areas in Montana were selected (Figure 2), on which a large number of field measurements were available, and that exhibited a range of regrowth conditions.

Unfortunately, Sentinel-1 data available in the ESA archives for these areas were limited, due to the acquisition strategy. As a consequence, we had to identify new study areas, prioritizing regions where Sentinel-1 acquisitions are much more frequent, due to research interest on interferometric use of SAR (InSAR) acquisitions, such as earthquake prone regions.

Potential areas were identified by cross referencing the MTBS database of historical fire perimeters (Eidinshink, 2007) with the Sentinel-1 Archive. Among the possible burned areas, the California King Fire (Ignition date: 13 September 2014) was selected because of the availability of pre-and post fire airborne optical and LiDAR data, that would compensate for the absence of USFS measurements.



Area 1: 15 x 15 km --> 11 siti di misura
 Area 2: 15 x 15 km --> 11 siti di misura



Area 3 (East of Missoula) : 10 x 5 km --> 6 measurements sites
 Area 4 (SouthWest of Missoula) : 10 x 5 km --> 14 measurements sites
 Area 5 (SouthEast of Missoula) : forest clearcutting as large square areas

Figure 2: Initial selection of the study sites, selected because of the availability of repeated ground measurements collected by the US Forest Service. Because of the limited availability of Sentinel-1A data, the sites could not be used and a new study area was identified.

3. Description of the study area

The King Fire, which ignited on September 13, 2014 due to arson, affected almost 400 km² in the Sierra Nevada Mountains (El-Dorado County, California) as illustrated in Figure 3.

The fire affected a mostly forested area, included in part in the El Dorado National Forest, and in part on privately owned land. The fire lasted over a month, and it resulted in extreme tree mortality on most of its extent (Figure 5: USFS damage assessment).

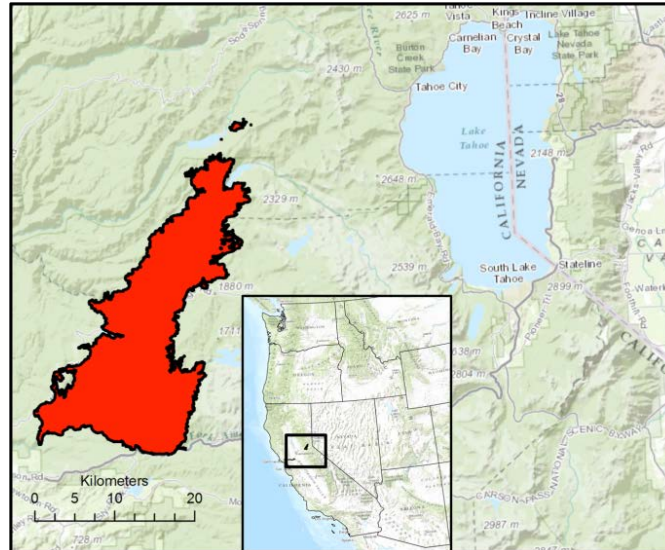


Figure 3: Geographic location of the King Fire

The area burned had been fortuitously covered in 2013 by an extensive airborne remote sensing campaign by NASA. Because of the extreme ecological impact of the King fire, the airborne measurements were repeated in 2015, resulting in an unique dataset of high resolution, multi-sensor airborne data collected shortly before and after one of the largest forest fires of the Western United States.

4 Available Datasets

4.1 Optical Remotely Sensed Datasets

The NASA JPL pre and post-fire airborne acquisitions include:

- AVIRIS: hyperspectral (224 bands), 0.4 to 2.4 μm spectral range, 14.8m spatial resolution
- MASTER: multispectral (49 bands, matching the ASTER space-borne instrument), 0.4 to 12.05 μm spectral range, 35m spatial resolution
- LiDAR, point cloud data converted to 30m canopy cover, intensity and topography metrics.

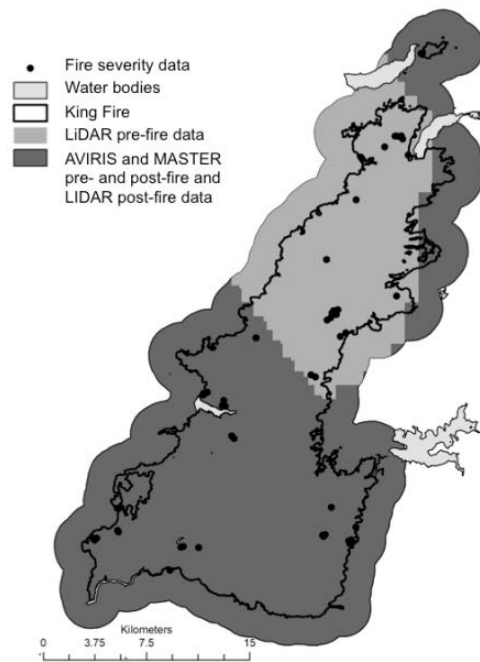


Figure 4: coverage of the airborne datasets. From JPL-NASA (<http://wildfire.jpl.nasa.gov/data/>)

Pre-fire data were collected on September 19, 2013, (MASTER, AVIRIS) and 20 March 2013 (LiDAR); post fire data on September 19, 2014 (MASTER) November 17, 2014 (MASTER, AVIRIS), 15 Jan 2015 (LiDAR). Data coverage is reported in Figure 4.

Reflectance measurements for the **spectroscopic AVIRIS** (an imaging spectrometer spanning the visible to shortwave infrared 0.38–2.5 μm) and **MASTER** (MODIS-ASTER airborne) sensors are distributed as multi-band *geotiffs* for the megafire and acquisition date.

Derived operational metric products for each sensor are provided in individual GeoTIFFs. GeoTIFFs produced from **LiDAR** (spatial resolutions of pixels from 1×1 m to 35×35 m) point data depict first order topographic indices and summary statistics of vertical vegetation structure.

Moreover King Fire was studied from **Landsat 8** satellite images.

These data are generated as part of the Monitoring Trends in Burn Severity (**MTBS**) project. MTBS is project conducted through a partnership between the U.S. Geological Survey National Center for Earth Resources Observation and Science (EROS) and the USDA Forest Service Remote Sensing Applications Center (RSAC)

CA3878212060420140913 (KING)

Latitude: $38^{\circ} 55' 48.0''$

Longitude: $-120^{\circ} 32' 31.2''$

Fire Ignition Date: September 13, 2014

Assessment Type: Extended

Pre-Fire Image Date: July 30, 2013 (Landsat 8)

Post-Fire Image Date: August 05, 2015 (Landsat 8)

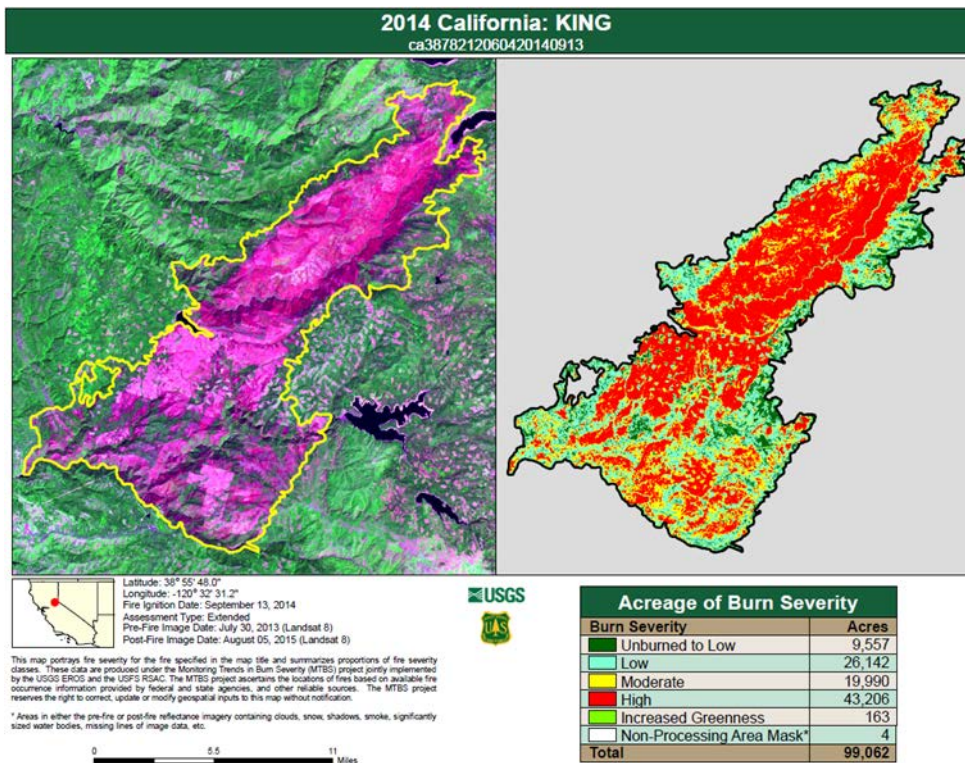


Figure 5: King fire datasheet. Source: US Forest Service

4.2 Sentinel-1 SAR data

The ESA Sentinel Hub contained, at the time of the performance of the project, 30 images covering the area. All **Sentinel-1A** (28 images) and **Sentinel-1B** (2 images) data were downloaded (SLC format) to a processing server at University of Idaho.

Table 2: List of Sentinel-1 data downloaded

Sentinel-1 Ascending

	ID	Pol	Orig	Process	Date	Sat
1	EA32	VV/VH	SLC	GRD	2016/05/13	S1A
2	A7AA	VV	SLC	GRD	2015/11/15	S1A
3	F626	VV	SLC	GRD	2016/01/31	S1A
4	26B9	VV	SLC	GRD	2016/02/19	S1A
5	D444	VV	SLC	GRD	2016/04/07	S1A
6	399D	VV	SLC	GRD	2016/05/01	S1A
7	4163	VV	SLC	GRD	2016/05/25	S1A
8	BED0	VV	SLC	GRD	2016/08/05	S1A
9	4DCB	VV	SLC	GRD	2016/09/22	S1A
10	7CA1	VV/VH	SLC	GRD	2016/11/03	S1B
11	BAE3	VV	SLC	GRD	2016/10/10	S1B

Sentinel-1 Descending

	ID	Pol	Orig	Process	Date	Sat
1	9D95	VV	SLC	GRD	2015/11/20	S1A
2	225D	VV	SLC	GRD	2015/12/14	S1A
3	A30A	VV	SLC	GRD	2016/01/07	S1A
4	94F3	VV	SLC	GRD	2016/01/31	S1A
5	CB68	VV	SLC	GRD	2016/01/31	S1A
6	285E	VV	SLC	GRD	2016/02/24	S1A
7	A420	VV	SLC	GRD	2016/03/19	S1A
8	552B	VV	SLC	GRD	2016/04/12	S1A
9	A1C7	VV	SLC	GRD	2016/05/06	S1A
10	D5D7	VV	SLC	GRD	2016/05/30	S1A
11	4411	VV	SLC	GRD	2016/08/10	S1A

Sentinel-1 Partial Cover (Ascending)

	ID	Pol	Orig	Process	Date	Sat
1	+7536	VV/VH	SLC	GRD	2016/03/14	S1A
2	9345	VV/VH	SLC	GRD	2016/03/14	S1A
3	3A8A	VV/VH	SLC	GRD	2016/08/29	S1A

Dual Pol acquisition List

Only 5 images were acquired in Dual Polarization (VV-VH).

IDs 9345 (3) and 7536 (4) should be mosaicked to get full cover same date (14 Mar 2016).

ID 3A8A (5) covers only very small part of King Fire study area.

	ID	Pol	Orig	Process	Date	Sat	Study area
1	EA32	VV/VH	SLC	GRD	2016/05/13	S1A	full
2	7CA1	VV/VH	SLC	GRD	2016/11/03	S1B	full
3	9345	VV/VH	SLC	GRD	2016/03/14	S1A	partial
4	7536	VV/VH	SLC	GRD	2016/03/14	S1A	partial
5	3A8A	VV/VH	SLC	GRD	2016/08/29	S1A	partial

5. Sentinel 1 data preprocessing

A processing chain was defined for the pre-processing of Single Look Complex Sentinel data to reprojected Ground Range Detected (GRD) using the Sentinel Application Platform (SNAP) toolbox provided by the European Space Agency.

The processing steps are as follows:

- Application of the orbit file
- Thermal Noise Removal
- Calibration
- TOPSAR-Deburst
- Multilook Merge
- Speckle Filtering
- Conversion to GRD
- Terrain Correction
- Conversion to 16 bit
- Reprojection to UTM/WGS 84, 20m resolution

6. Data Analysis

6.1 LiDAR

LiDAR point cloud datasets consist in point measurement of distance between the Canopy cover is the area of ground covered by a vertical projection of the canopy. It can also be defined as the proportion of the sky hemisphere obscured by vegetation when viewed from a single point.

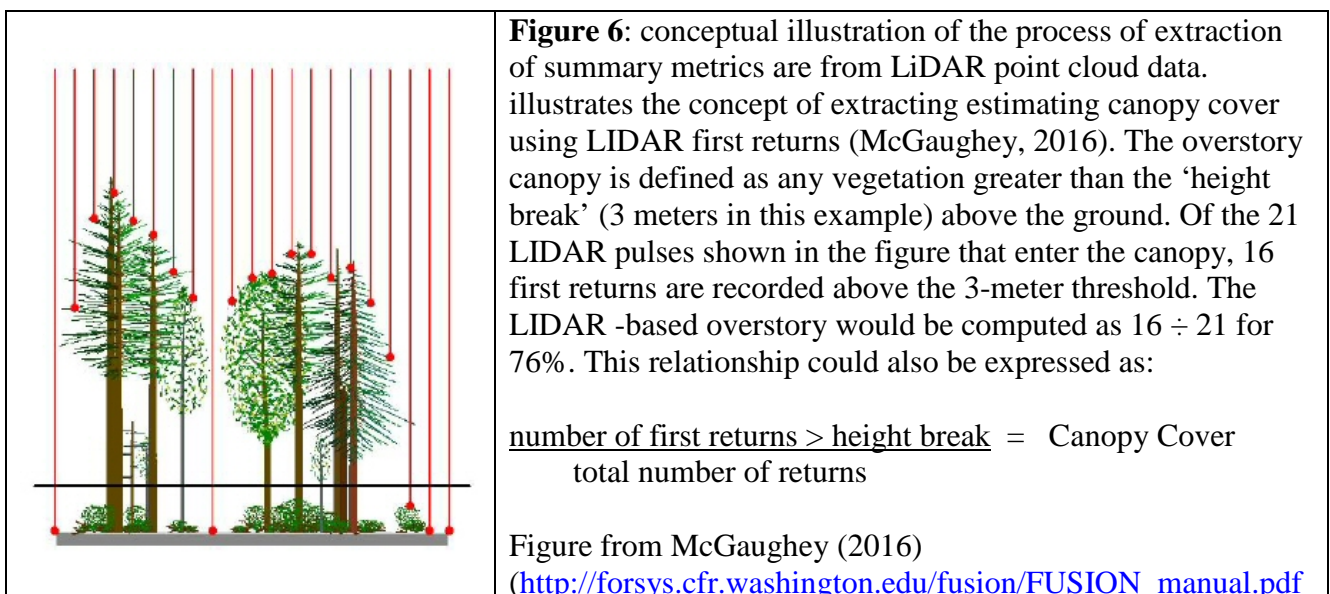
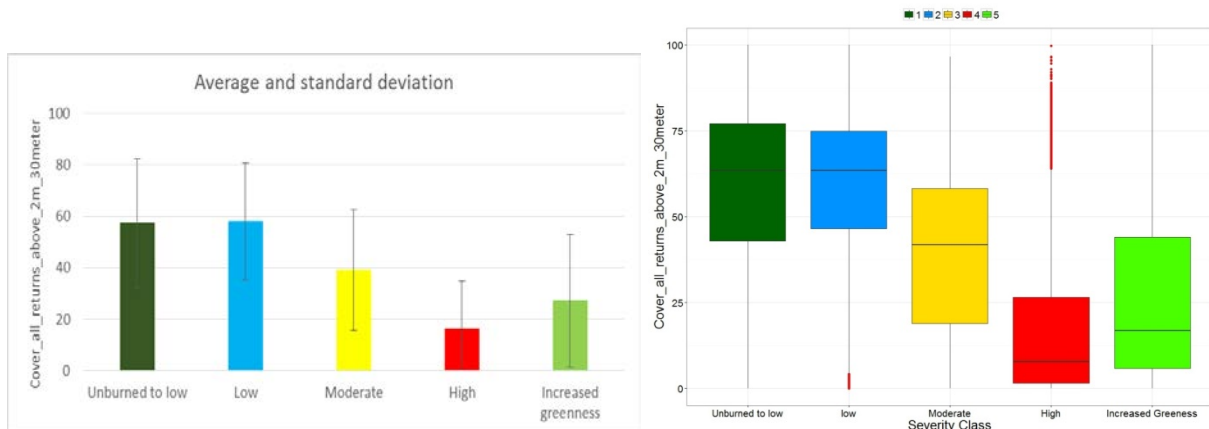


Table 2. Frequency of the MTBS severity classes within the perimeter of the King Fire burned area.

MTBS SEVERITY CLASS	NUMBER OF PIXELS	PERCENTAGE OF THE KING FIRE AREA
UNBURNED TO LOW	45 435	10%
LOW	118 043	26%
MODERATE	89 962	20%
HIGH	194 307	43%
INCREASED GREENNESS	789	0%
MASKED	24	0%
TOTAL	448 560	

Table 3. Cross tabulation of the “Cover_all_returns_above_2m_30meter“ metric by MTBS severity classes within the perimeter of the King Fire burned area.

MTBS SEVERITY CLASS	MIN	MAX	AVERAGE	STDEV
UNBURNED TO LOW	0	100	57.35925	25.09761
LOW	0	100	57.8906	22.80237
MODERATE	0	96.59	39.07564	23.6016
HIGH	0	99.74	16.15041	18.59067
INCREASED GREENNESS	0	100	27.1094	25.82552
MASKED	0	84.33	23.13259	30.14178

**Figure 6.** Box-plots showing the statistics of the “Cover_all_returns_above_2m_30meter” parameter for the MTBS burn severity classes over the King Fire, California. In each boxplot, the median value is the central bold line, extremes of the rectangle area are given by the first (Q1) and third (Q3) quartiles, whiskers are $Q1-1.5 \cdot IQR$ and $Q3+1.5 \cdot IQR$, where IQR is the inter-quartile range ($Q3 - Q1$), red dots are the outliers.

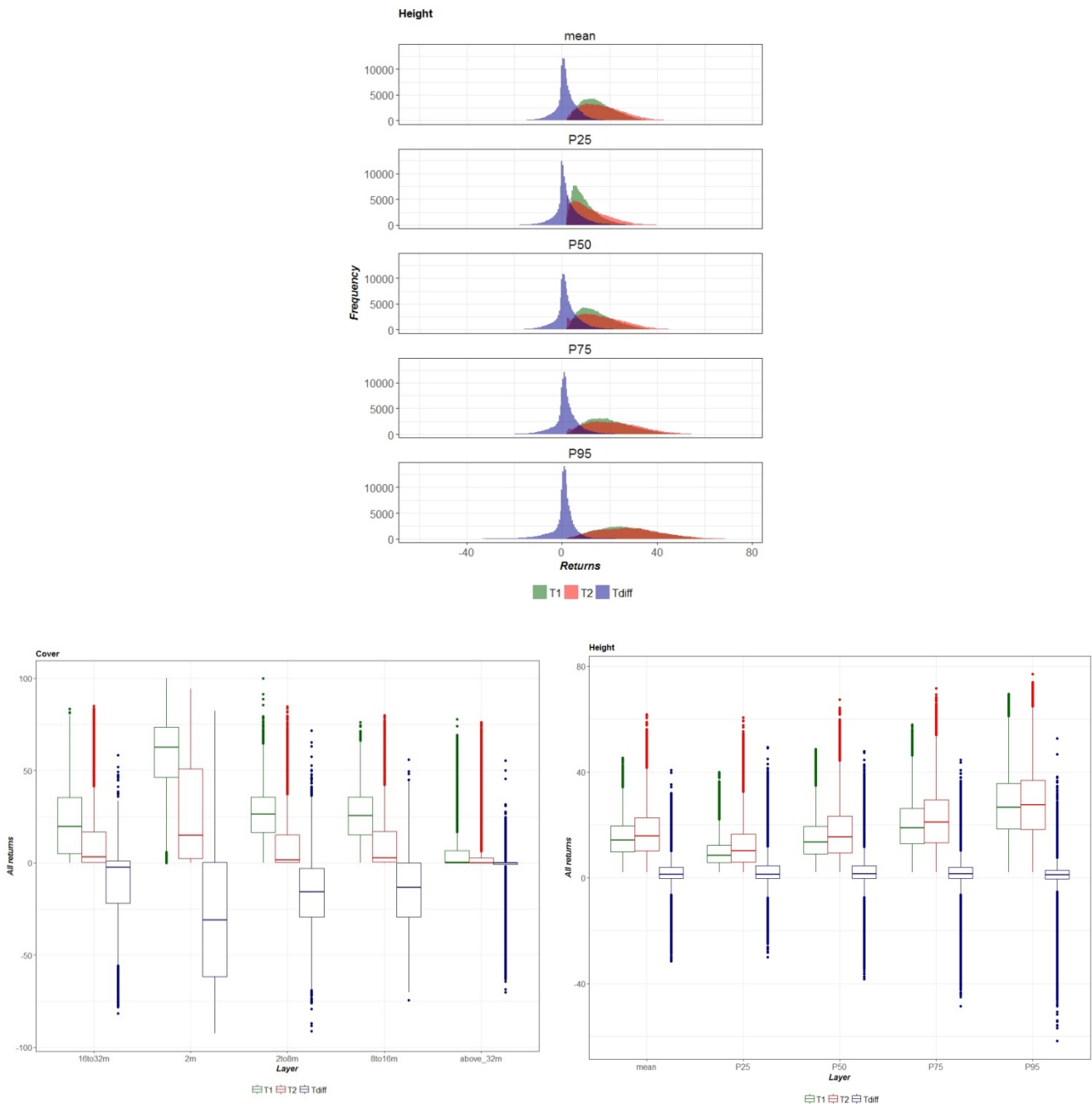


Figure 7 Multitemporal analysis of the pre-fire and post-fire LiDAR summary metrics, stratified by MTBS severity class. The plots show that high severity fire areas are characterized by decrease in canopy cover, and relatively unchanged maximum height. This is consistent with crown fires that cause the loss of twigs and branches, while the trunk of the trees remains standing.

Upper left: histogram of the distribution of the height metric.

Lower left: box-plot of the distribution of the height metric.

Lower right: box-plot of the distribution of the coverage metrics.

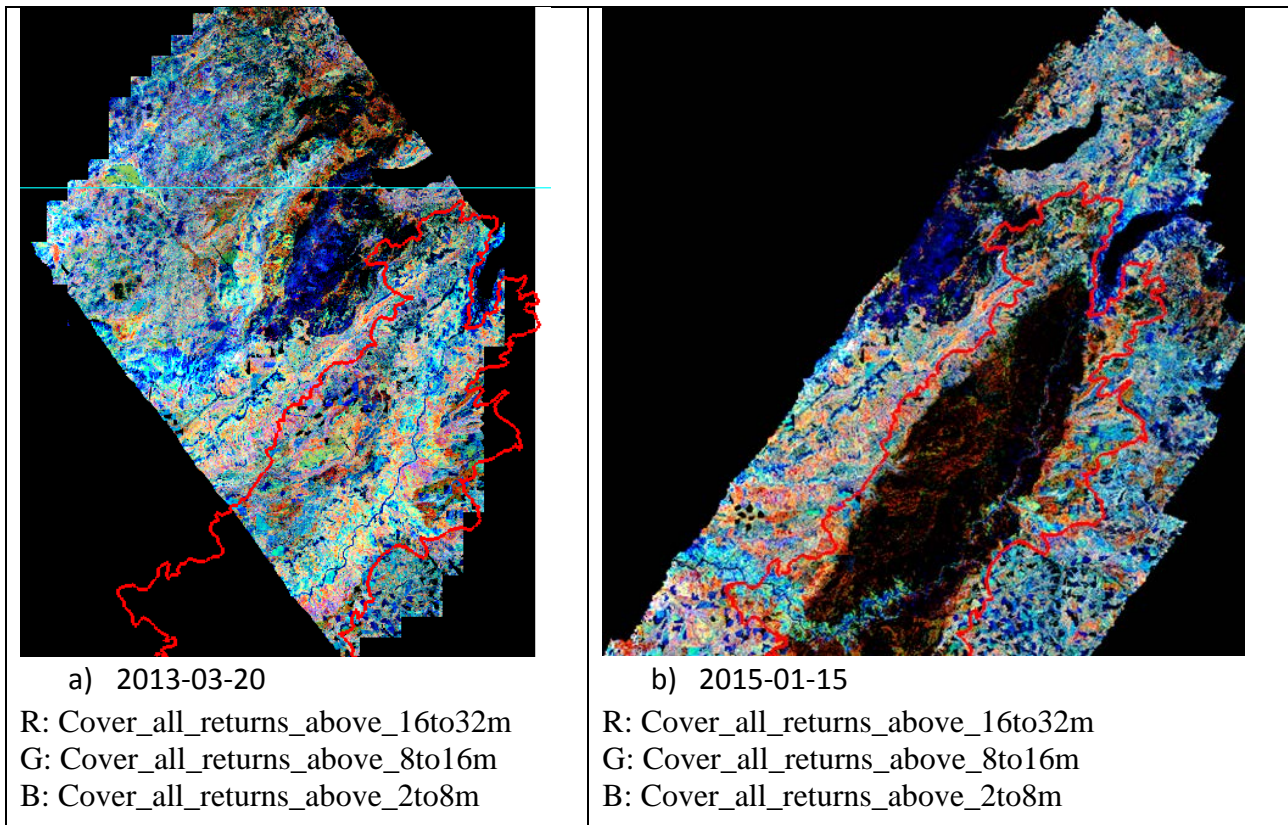


Figure 8 - RGB composite of KingFire_LIDAR_L2v1 (30 m) from (a) pre-fire acquisition (2013-03-20) and (b) post fire acquisition (2015-01-15).

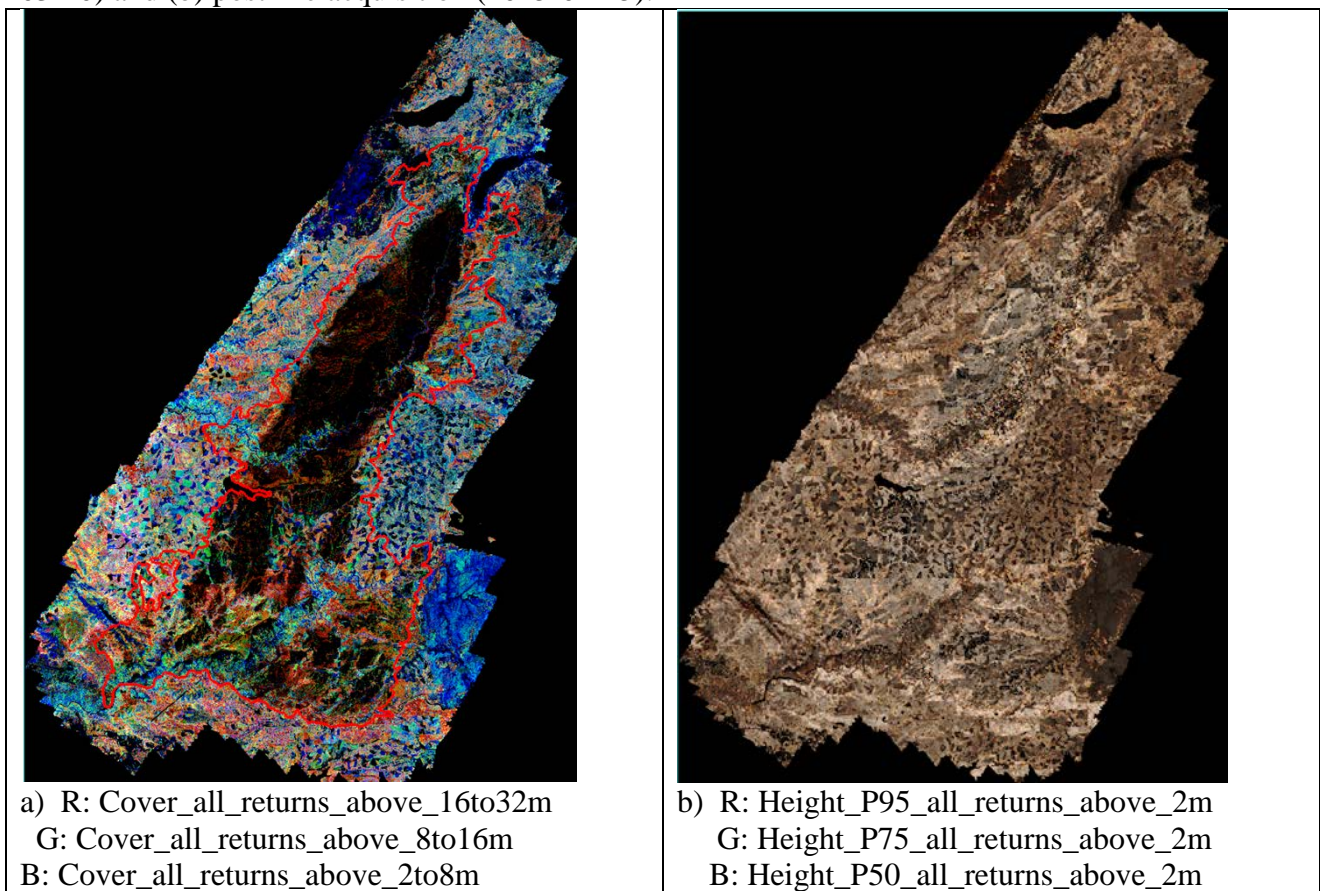


Figure 9 - RGB composite of KingFire_LIDAR_20150115_L2v1 (30 m) from post fire acquisition (2015-01-15) from Cover returns (a) and Height returns (b).

6.2 MASTER (MODIS-Aster)

Fire Ignition Date: **September 13, 2014**

Acquisition dates: September 19, 2013 / September 19, 2014 (smoke) / November 17 2014

Table 4. Spectral channels of MASTER data downloaded correspond with 6 spectral bands of Landsat-8 OLI

MASTER spectral bands (central peak)	Landsat-8 OLI spectral bands (interval)
ch2 (0.496) → Blue	b2 0.45 – 0.51
ch3 (0.538) → Green	b3 0.53 – 0.59
ch5 (0.652) → Red	b4 0.64 – 0.67
ch9 (0.866) → NIR	b5 0.85 – 0.88
ch12 (1.608) → SWIR1	b6 1.57 – 1.65
ch22 (2.212) → SWIR2	b7 2.11 – 2.29

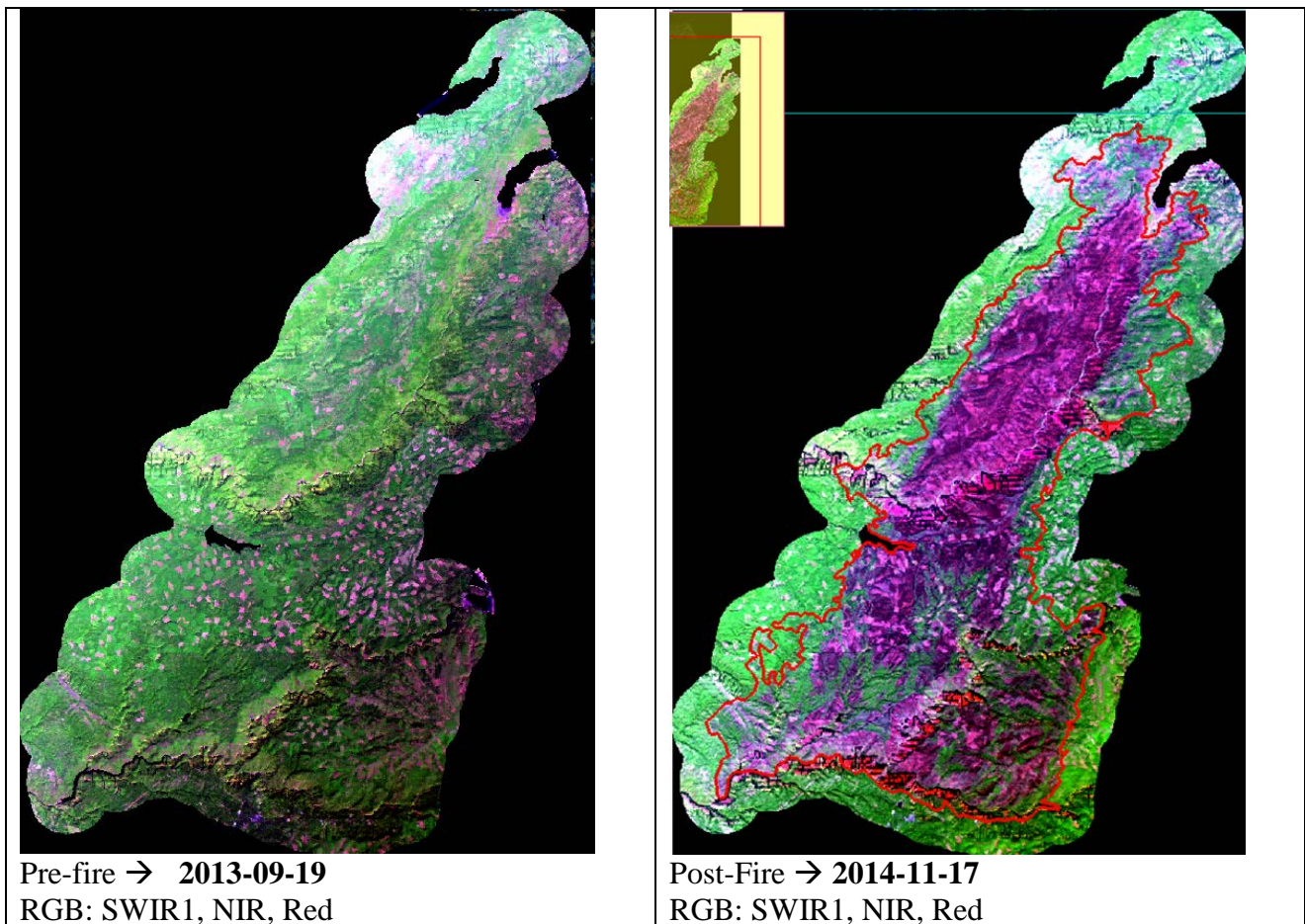


Figure 10 - RGB: SWIR1, NIR, Red composite of King Fire from MASTER (30 m) from (a) pre-fire acquisition (2013-09-19) and (b) post fire acquisition (2014-11-17). Fire perimeter from MTBS

6.3 Sentinel 1 SAR

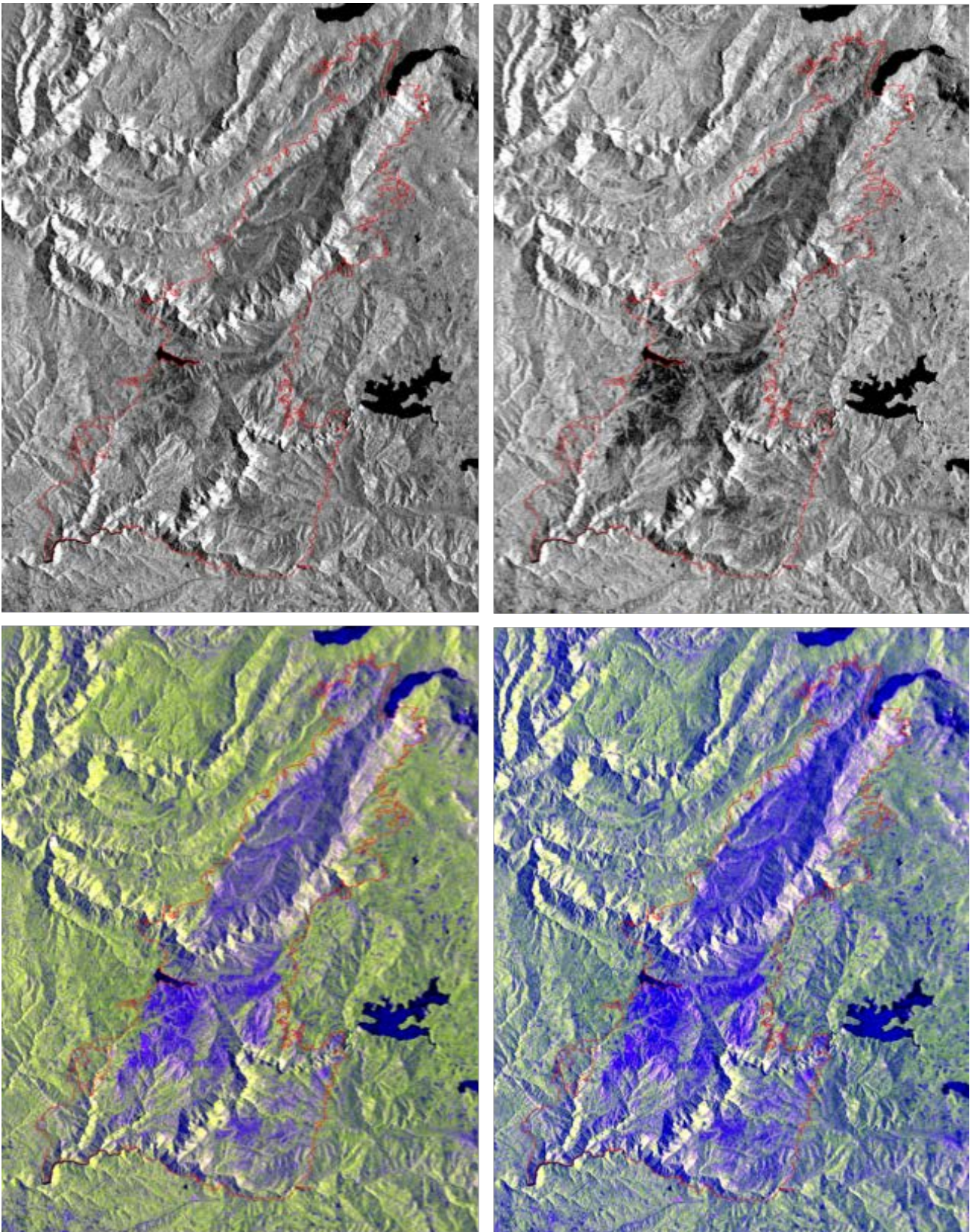


Figure 11 –Sentinel 1 SAR image of the King Fire, acquired on May 13, 2016.

Upper left: backscatter intensity, VV polarization. *Upper right:* backscatter intensity, VH polarization.

Lower left: RGB composite of VV backscatter (red), VH backscatter (green), VV/VH ratio (blue).

Lower right: RGB composite of VV backscatter (red), VH backscatter (green), forest damage index (blue).

The analysis of Sentinel-1A and Sentinel 1B images of the King fire was consistent with the previous literature on SAR C band burned area characterization. While it was not possible to compare pre-fire and post fire imagery due to the fact that the King fire pre-dates the launch of Sentinel-1A, after the fire high severity areas (Figure 11) are characterized by a decrease both in the intensity of the backscatter in VV polarization and VH polarization, but the decrease is greater in VH polarization. This is due to the fact that VH polarization is sensitive to double bounces of the radar pulses, which are less frequent as part of the structure of the forest is removed by the fire.

Previous literature (Tanase et al., 2014, 2015, 2016, Verhegghen et al., 2016) suggests that the structural forest changes can be detected by the ratio between VV and VH polarization, or by the Radar Forest Degradation Index (RDFI),

$$\mathbf{RDFI} = (\mathbf{VV-VH}) / (\mathbf{VV+VH})$$

proposed by Mitchard et al. (2011).

7. Next steps

The preliminary analysis performed during the project, necessarily limited by the short temporal duration of the activities, showed that Sentinel 1A SAR data can be combined with optical datasets to characterize the post-fire status of burned areas in forest environments.

The collaboration will continue in the next months, to expand the analysis, publish the results, and explore potential sources of funding for a follow-up proposal.

Future activities will focus on:

- Expansion of the analysis to a second fire in California (Rim Fire) also covered by pre-fire and post-fire LiDAR and optical airborne datasets made available by NASA-JPL, with the objective of testing if the same behavior of the Sentinel-1 data can be observed.
- Quantitative comparison of LiDAR and radar metrics, and investigating the availability of ground measurements (contacts with the US Forest Service are underway at the time of writing).
- Publication of the results in peer reviewed international journals.

References

Boschetti, L., Roy, D. P., Justice, C. O., & Humber, M. L. (2015). MODIS–Landsat fusion for large area 30m burned area mapping. *Remote Sensing of Environment*, 161, 27-42.

De Santis, A., & Chuvieco, E. (2009). GeoCBI: A modified version of the Composite Burn Index for the initial assessment of the short-term burn severity from remotely sensed data. *Remote Sensing of Environment*, 113(3), 554-562.

Dickinson, M. B., & Johnson, E. A. (2001). Fire effects on trees. Forest fires: behavior and ecological effects. Edited by EA Johnson and K. Miyanishi. Academic Press, New York, 477-525.

- Giglio, L., Descloitres, J., Justice, C. O., & Kaufman, Y. J. (2003). An enhanced contextual fire detection algorithm for MODIS. *Remote Sensing of Environment*, 87(2), 273-282.
- Dobson, M. C., Ulaby, F. T., LeToan, T., Beaudoin, A., Kasischke, E. S., & Christensen, N. (1992). Dependence of radar backscatter on coniferous forest biomass. *IEEE Transactions on Geoscience and Remote Sensing*, 30(2), 412-415.
- Eidenshink, J., Schwind, B., Brewer, K., Zhu, Z. L., Quayle, B., & Howard, S. (2007). Project for monitoring trends in burn severity. *Fire ecology*.
- Hook, S. J. Myers, J. J., Thome, K. J., Fitzgerald, M. and A. B. Kahle, 2001. The MODIS/ASTER airborne simulator (MASTER) - a new instrument for earth science studies. *Remote Sensing of Environment*, vol. 76, Issue 1, pp. 93-102.
- Hudak, A. T., Evans, J. S., & Stuart Smith, A. M. (2009). LiDAR utility for natural resource managers. *Remote Sensing*, 1(4), 934-951.
- Imhoff, M. L. (1995). A theoretical analysis of the effect of forest structure on synthetic aperture radar backscatter and the remote sensing of biomass. *IEEE Transactions on Geoscience and Remote Sensing*, 33(2), 341-352.
- Kasischke, E. S., Turetsky, M. R., Ottmar, R. D., French, N. H., Hoy, E. E., & Kane, E. S. (2008). Evaluation of the composite burn index for assessing fire severity in Alaskan black spruce forests. *International Journal of Wildland Fire*, 17(4), 515-526.
- Key, C. H., & Benson, N. C. (1999). The composite burn index (CBI): field rating of burn severity. USGS, NRMSC research,[online] Available: <http://nrmsc.usgs.gov/research/cbi.htm> [3/14/2006].
- Kurum, M. (2015). C-Band SAR Backscatter Evaluation of 2008 Gallipoli Forest Fire. *IEEE Geoscience and Remote Sensing Letters*, 12(5), 1091-1095.
- Le Toan, T., Beaudoin, A., Riou, J., & Guyon, D. (1992). Relating forest biomass to SAR data. *IEEE Transactions on Geoscience and Remote Sensing*, 30(2), 403-411.
- Malenovský, Z., Rott, H., Cihlar, J., Schaepman, M. E., García-Santos, G., Fernandes, R., & Berger, M. (2012). Sentinels for science: Potential of Sentinel-1,-2, and-3 missions for scientific observations of ocean, cryosphere, and land. *Remote Sensing of Environment*, 120, 91-101.
- Martins, F. D. S. R. V., dos Santos, J. R., Galvão, L. S., & Xaud, H. A. M. (2016). Sensitivity of ALOS/PALSAR imagery to forest degradation by fire in Northern Amazon. *International Journal of Applied Earth Observation and Geoinformation*, 49, 163-174.
- McGaughey, R., 2016 FUSION/LDV: Software for LIDAR Data Analysis and Visualization (http://forsys.cfr.washington.edu/fusion/FUSION_manual.pdf; page 49)
- Mitchard, E. T. A., Saatchi, S. S., White, L. J. T., Abernethy, K. A., Jeffery, K. J., Lewis, S. L., ... & Meir, P. (2011). Mapping tropical forest biomass with radar and spaceborne LiDAR: overcoming problems of high biomass and persistent cloud. *Biogeosciences Discussions*, 8(4), 8781.

- C. Pohl, J. L. van Genderen, 1998 Multisensor image fusion in remote sensing: concepts, methods and applications, *International Journal of Remote Sensing*, 19 5 (March 1998), 823-854 . 0143-1161
- Potter et al. (2012) Analysis of sapling density regeneration in Yellowstone National Park with hyperspectral remote sensing data. *Remote Sensing of Environment* **121**: 61-68.
- Roy, D. P., Boschetti, L., & Trigg, S. N. (2006). Remote sensing of fire severity: assessing the performance of the normalized burn ratio. *IEEE Geoscience and Remote Sensing Letters*, 3(1), 112-116.
- Roy, D. P., Boschetti, L., Justice, C. O., & Ju, J. (2008). The collection 5 MODIS burned area product—Global evaluation by comparison with the MODIS active fire product. *Remote Sensing of Environment*, 112(9), 3690-3707.
- Saatchi, S., Agosti, D., Alger, K., Delabie, J., & Musinsky, J. (2001). Examining fragmentation and loss of primary forest in the southern Bahian Atlantic forest of Brazil with radar imagery. *Conservation Biology*, 15(4), 867-875.
- Schroeder, W., Oliva, P., Giglio, L., & Csiszar, I. A. (2014). The New VIIRS 375m active fire detection data product: Algorithm description and initial assessment. *Remote Sensing of Environment*, 143, 85-96.
- Schroeder, W., Oliva, P., Giglio, L., Quayle, B., Lorenz, E., & Morelli, F. (2016). Active fire detection using Landsat-8/OLI data. *Remote Sensing of Environment*, 185, 210-220.
- Smith, A. M., Sparks, A. M., Kolden, C. A., Abatzoglou, J. T., Talhelm, A. F., Johnson, D. M., Boschetti L., Tinkham, W. T. (2016). Towards a new paradigm in fire severity research using dose-response experiments. *International Journal of Wildland Fire*, 25(2), 158-166.
- Stavros, E.N., T. Zachary, V. Kane, S. Veraverbeke, R. McGaughey, J. Lutz, C. Ramirez, & D.S. Schimel (2016) Unprecedented remote sensing data over the King and Rim Megafires in the Sierra Nevada Mountains of California. *Ecology*.
- Stroppiana, D., G. Bordogna, P. Carrara, M. Boschetti, L. Boschetti, and P.A. Brivio (2012). A method for extracting burned areas from Landsat TM/ETM+ images by soft aggregation of multiple Spectral Indices and a region growing algorithm. *ISPRS Journal of Photogrammetry and Remote Sensing*, 69, 88-102.
- Stroppiana, D., R. Azar, F. Calò, A. Pepe, P. Imperatore, M. Boschetti, J.M.N. Silva, P.A. Brivio, R. Lanari, (2015). Integration of Optical and SAR Data for Burned Area Mapping in Mediterranean Regions. *Remote Sensing* 2015, 7(2),1320-1345
- Tanase, M. A., Kennedy, R., & Aponte, C. (2015a). Radar burn ratio for fire severity estimation at canopy level: An example for temperate forests. *Remote Sensing of Environment*, 170, 14-31.
- Tanase, M. A., Kennedy, R., & Aponte, C. (2015b). Fire severity estimation from space: a comparison of active and passive sensors and their synergy for different forest types. *International Journal of Wildland Fire*, 24(8), 1062-1075.

Tanase, M. A., Santoro, M., Aponte, C., & de la Riva, J. (2014). Polarimetric properties of burned forest areas at C-and L-band. *IEEE Journal of Selected Topics in Applied Earth Observations and Remote Sensing*, 7(1), 267-276.

Tansey, K., Grégoire, J. M., Stroppiana, D., Sousa, A., Silva, J., Pereira, J., ... & Flasse, S. (2004). Vegetation burning in the year 2000: Global burned area estimates from SPOT VEGETATION data. *Journal of Geophysical Research: Atmospheres*, 109(D14).

Torres, R., Snoeij, P., Geudtner, D., Bibby, D., Davidson, M., Attema, E., ... & Traver, I. N. (2012). GMES Sentinel-1 mission. *Remote Sensing of Environment*, 120, 9-24.

Verhegghen, A., Eva, H., Ceccherini, G., Achard, F., Gond, V., Gourlet-Fleury, S., & Cerutti, P. O. (2016). The potential of sentinel satellites for burnt area mapping and monitoring in the Congo Basin forests. *Remote Sensing*, 8(12), 986.